Chapter 11
Temperature and Heat Transfer Measurements

Cengiz Camci
Turbomachinery Aero-heat Transfer Laboratory, The Pennsylvania State University, University Park, PA, USA

1 INTRODUCTION

Temperature is an important parameter for aerospace engineering system design. There are a great number of aerospace systems failing mainly because of thermal reasons. Satellite thermal management systems, hot sections of propulsion systems, combustors, aerodynamic heating of supersonic/hypersonic vehicle surfaces, turbomachinery flow simulators, jet engine demonstrators, composite manufacturing facilities, and rocket engines – all require a large number of sensors that can measure temperature and heat flux with acceptable accuracy.

All materials in aerospace engineering systems consist of atoms and/or molecules existing in a more or less agitated thermodynamic state. Whether materials are in a solid, liquid, or gaseous phase is related to the level of agitation. The cohesive forces binding the particles together are usually balanced by the kinetic energy of the individual particles. Temperature in a material can be regarded as the degree of activity attained by the particles in the system. Thus the concept of temperature in empty space is not meaningful, since there are no agitated particles in empty space. A body in which "thermal agitation" is totally absent is said to have an absolute temperature of zero.

The most direct realization of a scale of temperature using this approach is based on the ideal gas equation (Rogers and Mayhew, 1983). The ideal gas equation $p = \rho RT$ gives the static pressure p of a gas at a density ρ and static temperature T, with a gas constant R which is equal to the number of molecules in the specific volume divided by Boltzmann's constant κ. The constant volume gas thermometer, in which the pressure of a fixed mass of an inert ideal gas is measured as a function of temperature, uses this approach. It forms the basis of most temperature measurement schemes.

An "International Temperature Scale" is used by the scientific community. According to the zeroth law of thermodynamics, "two systems in thermal equilibrium with a third system are in thermal equilibrium with each other". The operational temperature scale is defined using a series of fixed reference points such as boiling and freezing points. Temperature cannot be measured directly, but has to be quantified by observing the effect it produces, such as the expansion of a liquid, the electrical current it induces in a bi-metallic junction, the color change it causes in a liquid crystal coating, etc. In general, assumptions need to be made about the linearity of the effect observed.

Most electronic temperature sensors used in engineering are either resistive or thermoelectric (Turner and Hill,

Encyclopedia of Aerospace Engineering.
Edited by Richard Blockley and Wei Shyy
 ISBN: 978-0-470-75440-5

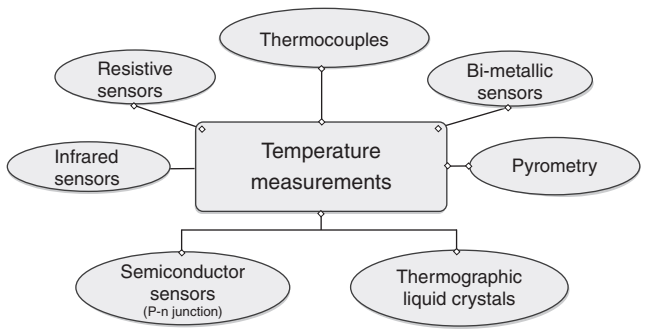

Figure 1. A general classification of the most frequently used temperature sensors in aerospace engineering.

1999). Resistive sensors may be either metallic or semiconductor based. Thermoelectric sensors or thermocouples are self-generating, but their very low output at μV level almost always requires an amplifier in the measurement chain. The thermal expansion of a solid or a bi-metallic system can also be used as a temperature transducer. Infrared emission or pyrometry can be instrumental in temperature sensing, and is particularly useful in the non-intrusive monitoring of inaccessible or rotating components.

A general classification of temperature sensors is shown in Figure 1. The last section of this chapter deals with heat transfer measurements in aerospace engineering. These systems measure the rate of thermal energy transferred from one point to another in a domain filled with a gas, solid, or liquid material.

2 RESISTIVE TEMPERATURE TRANSDUCERS

Resistive temperature detectors (RTDs) based on metals or semiconductors are probably the most common type in use. The semiconductor versions are the most frequently used and probably the cheapest. Metallic resistive temperature sensors offer better performance than semiconductor RTDs and may be installed when high accuracy is required.

2.1 Metallic resistive temperature sensors

Metallic resistive sensors often take the form of a non-inductively wound coil of a metallic wire such as platinum, copper, tungsten, or nickel. The coils may be encapsulated within a miniature sealed glass tube. Thin or thick films of metals can also be deposited on flexible Mylar substrates or quartz/ceramic substrates. In general, the resistance of the RTD can be adjusted by controlling the length-to-width ratio of the active resistive films. The variation of resistance R with respect to temperature T of most metallic materials can be represented by the equation

$$R = R_0(1 + \alpha_1 T + \alpha_2 T^2 + \alpha_3 T^3 + \cdots + \alpha_n T^n) \qquad (1)$$

where R_0 is the resistance at a user selected reference temperature T_0. Platinum, nickel, and copper are the most commonly used metals, and they generally require a summation containing at least α_1 and/or α_2 for accurate temperature measurements. In most aerospace engineering applications, it is often possible to model a metallic RTD using only one coefficient α_1. In a typical engineering application using only α_1, the resulting nonlinearity is only around 0.5% in a temperature range from -40 to $+140\,^{\circ}$C. The nominal resistance R_0 of a metallic RTD can vary from a few ohms to several kilohms. However, 100 Ω is a fairly standard value. The resistance change of a metallic RTD can be quite large and is typically up to 20% of the nominal resistance over the design temperature range.

2.2 Resistance temperature sensor (RTD) bridge circuits

Thermistors are modulating transducers that are normally used in a Wheatstone-balancing-bridge circuit as shown in Figure 2. While the resistance changes exhibited by a metallic RTD are reasonably linear, those shown by semiconductor thermistors are markedly nonlinear. In both cases, the resistance changes are large enough to record accurately.

Even if the sensor output is linear, the out-of-balance voltage measured using a bridge circuit is not necessarily linear when the sensor resistance varies significantly. The current through the sensor is usually in the range from 1 to 25 mA, resulting in Joule heating to take place in the sensor (Turner and Hill, 1999). This internal heat generation causes a "self-heating" error depending on the conduction and convection heat transfer characteristics of the substrate to which the sensor is attached. The four-wire "ohmmeter"

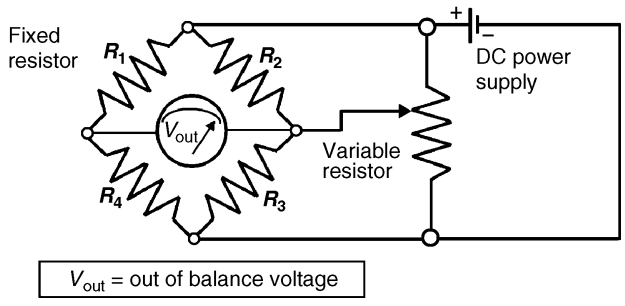

Figure 2. Bridge balancing arrangement for RTD sensors.

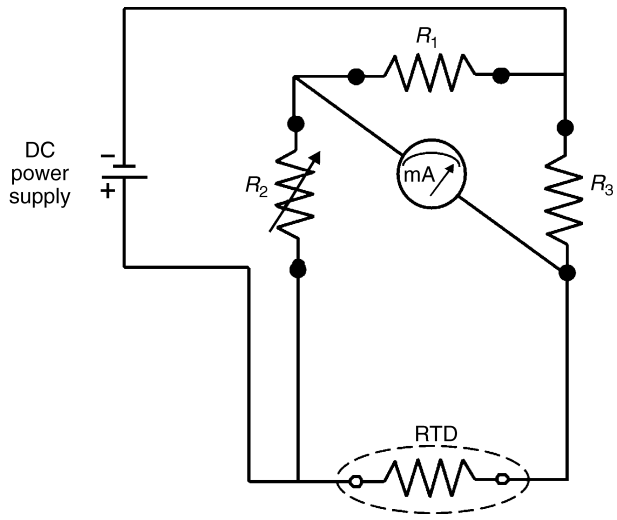

Figure 3. Four wire circuit for resistance thermometry.

technique shown in Figure 3 is an alternative to the classical bridge techniques for conditioning RTD sensors. This specific bridge circuitry is widely used with data acquisition systems having accurate A/D converters. Any sensor nonlinearity is corrected in the computer software after collecting data using either 12-2 bit or 16-2 bit A/D converters.

2.3 Thermistors

Thermistors are semiconductor-based transducers, manufactured in the shape of flat disc, beads, or rods. When two or more oxides of copper, cobalt, iron, manganese, nickel, magnesium, vanadium, tin, titanium, or zinc are combined, the resulting thermistor is said to have a negative temperature coefficient (NTC) of resistance. As the temperature goes up, the electrical resistance of the NTC thermistor falls. The accuracy of a thermistor is not as good as that of a metallic RTD, due to possible variations in the composition of the semiconductor inherent to its manufacturing technique. Thermistors are known to be nonlinear unlike metallic RTDs as expressed by equation (2). The resistance versus temperature relation is usually of the form:

$$R = R_0 \mathrm{e}^{\beta\left(\frac{1}{T} - \frac{1}{T_0}\right)} \tag{2}$$

where R_0 is the nominal resistance at temperature T_0, and β is a constant that is thermistor material dependent. The reference temperature T_0 is usually taken to be 298 K, and β is of the order of 4000. Thermistors can be used within the temperature range from -60 to $+\ 150\,^{\circ}$C with an accuracy as high as $\pm 0.1\%$. A thermistor has a very steep voltage response to varying temperature in a relatively narrow temperature interval. Positive temperature coefficient (PTC) thermistors can also be obtained by using materials such as barium, lead, or strontium.

3 THERMOCOUPLES

One of the most frequently used sensors for temperature measurements in aerospace systems is the thermocouple. Thermocouples can be very small, cost-effective, and remarkably accurate when used with a proper understanding of their characteristics (Arts and Charbonnier, 1994). The operational range of thermocouple-based measurements in aerospace systems is quite wide. While measurements in a liquid helium bath at a level of $-270\,^{\circ}$C are possible, temperatures in gas turbine combustors near 1500 °C are commonly encountered. It is possible to extend this measurement range up to 2200 °C for the case of high-temperature furnaces.

When two dissimilar metals are in contact with each other, a thermal load existing over the junction of the metallic couple induces a measurable electrical potential. A thermocouple is a self-generating transducer made up of two or more junctions. A conventional thermocouple temperature measurement arrangement is shown in Figure 4a. One junction (the cold junction) needs to be maintained at a known

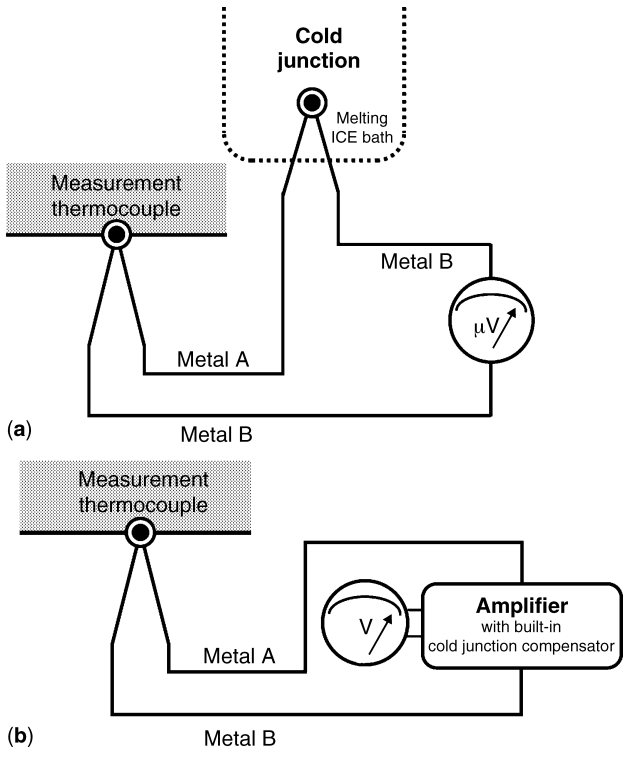

Figure 4. Conventional thermocouple arrangement: (a) standard approach with a cold junction (melting ice bath) and (b) with built-in junction compensator in the amplifier and signal conditioner.

reference temperature, for instance by surrounding it with melting ice. The other junction is attached to the object to be measured. A more practical circuit is shown in Figure 4b with the two wires directly connected to a measuring circuit containing a built-in cold junction compensator. The junctions between the two wires and the voltmeter do not cause any error signal to appear as long as they are at the same temperature. Since there is no proper reference junction with this approach, the system may give an erroneous output if the temperature of the surrounding environment changes. This small error may be avoided by using a cold junction compensation system. The operating characteristics of thermocouples were first observed by Seebeck in 1821. He measured a net electrical potential change when the junction of a bi-metallic couple is heated to a controlled temperature level. Peltier later showed that this effect was reversible. A bi-metallic thermocouple also showed a measurable temperature increase when a small electrical current was externally imposed on the junction.

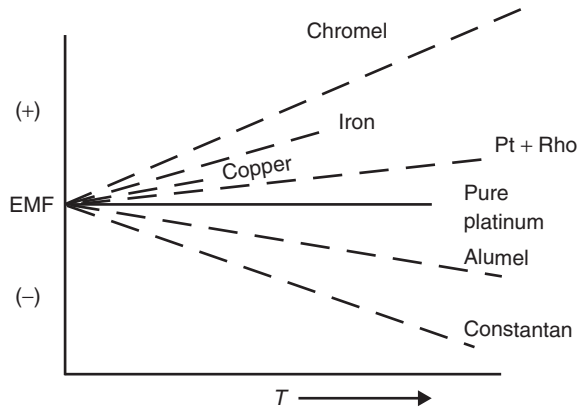

Figure 5. Electro-motor-force versus temperature for various thermocouple materials. Reproduced with permission from Arts and Charbonnier (1994). © von Karman Institute for Fluid Dynamics (2009).

3.1 Principle of operation of thermocouples

A summary of thermocouple measurement principles, basic laws of thermoelectricity, thermocouple compensation, possibility of spurious signal generation, thermopiles, and multiple thermocouple measurements will be discussed in the next few paragraphs. A comprehensive treatment of this topic can also be found in Arts and Charbonnier (1994) and Moffat (1962). Materials used in thermocouple manufacturing can be classified in terms of thermoelectric polarity which indicates the slope of the EMF versus junction temperature curve. A "positive" material produces an increase in measured EMF along its length in response to elevated temperature as shown in Figure 5. The slopes for materials are relative to pure platinum. A graphical description of the simplest possible basic thermocouple circuit is presented in Figure 6a. The circuit measures the temperature T_{HOT} relative to the ambient temperature T_{AMB} existing at the instrument terminals. The electrical potential V_{1-3} measured between the junctions 1 and 3 indicates the value of $(T_{HOT} - T_{AMB})$. If the measurement of T_{HOT} alone is desired, then the junction temperature at T_{AMB} must also be measured.

When a more accurate measurement of T_{HOT} is needed, a reference box is added to the measurement system as shown in Figure 6b. A reference box may contain an ice bath, a triple point, or an isothermal plate with precise temperature control in time. The temperature of the reference zone T_{REF} needs to be known precisely.

Another approach may be to electronically control the temperature of a reference block precisely, at a selected T_{REF}. Two different measurement circuits with a reference junction are possible. In Figure 6c, iron and constantan wires form junctions 2 and 4 when they are coupled with copper wires. The junctions 2 and 4 are both immersed in the reference box, which is precisely kept at T_{REF}. The small-magnitude EMF values generated between 1–2 and 4–5 do not contribute to the actual EMF measurement sampled at the ends of the copper wires V_{1-5}. The electrical voltage drop occurring between 1–2 and the voltage gain between 4–5 automatically cancel each other. The copper leads do not influence the overall measurement of V_{1-5}, which is now directly proportional to $(T_{HOT} - T_{REF})$. If the reference junction is a melting ice bath at $T_{REF} = 0.01\,^{\circ}\mathrm{C}$ then V_{1-5} is directly proportional to T_{HOT}.

The second thermocouple circuit approach with a reference junction is shown in Figure 6(c). This approach utilizes a second identical thermocouple without any copper connection. The second thermocouple is usually kept at a known reference temperature T_{REF}. Either the ice point or the triple point for water is used for this purpose. It should be noted that measured V_{1-2} and V_{4-5} are two different measured voltage changes.

3.2 Spurious signal generation in thermocouples

A thermocouple may always provide a signal unless the wires are not broken. Thermocouples are known to generate spurious signals if proper attention is not paid to a few of their important properties. Spurious EMFs are usually generated because of excessive AC electrical noise. Electrical ground loops may also result in erroneous signals. Other significant spurious EMF problems are galvanic EMF generation, strain-induced EMFs, and material inhomogeneities in a

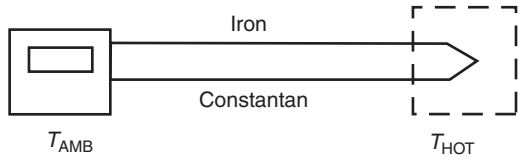

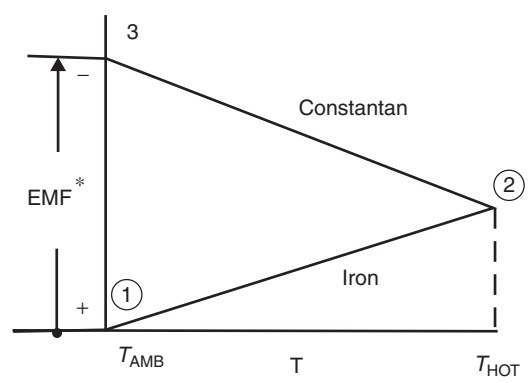

(**a**)

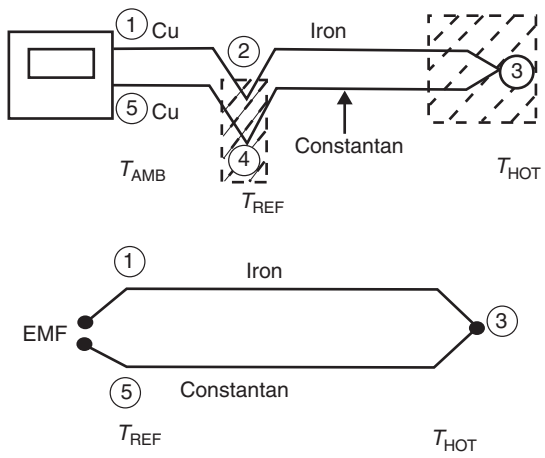

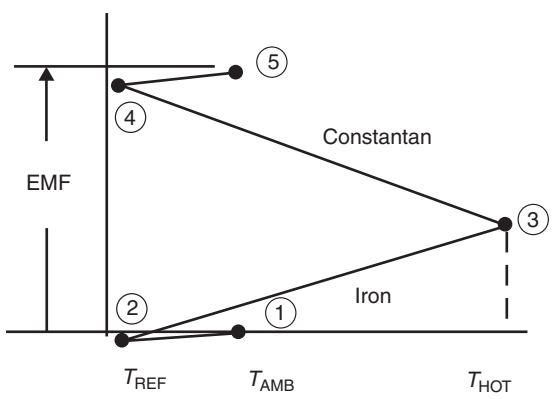

(**b**)

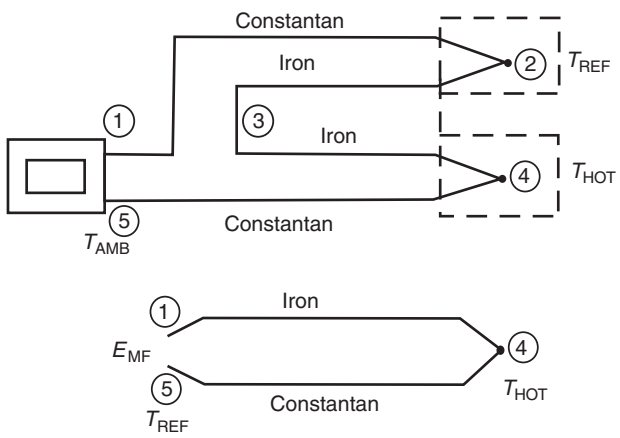

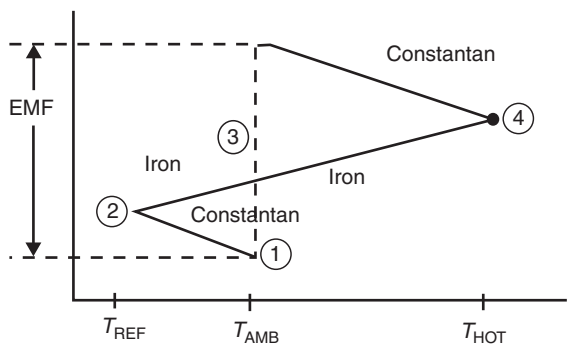

(**c**)

Figure 6. Various thermocouple connection schemes: (a) thermocouple measurements with no reference zone box, (b) measurements with a reference zone box using copper connectors and (c) measurements with a reference zone box – without copper connectors.

thermocouple circuit and in the junction areas (Arts and Charbonnier, 1994).

3.3 Laws of thermoelectricity for thermocouples

An understanding of thermocouples may be possible by referring to a set of "laws" given by various authors (Arts and Charbonnier, 1994).

Effect of intermediate temperature variation: *The thermal EMF of a thermocouple with junctions at T_1 and T_3 is totally unaffected by any temperature elsewhere in the circuit (i.e., T_2) if the two metals used are each homogeneous.*

Effect of a third homogeneous material in a thermocouple circuit: *If a third homogeneous metal C is inserted into either wire A or B as long as the two new thermo-junctions are at equal temperatures, the net EMF of the circuit is unchanged irrespective of the temperature of C away from the junctions.*

Effect of third homogeneous material at junction: *If metal C is inserted between A and B at one of the junctions, the temperature of C at any point away from the AC and BC junctions is immaterial. So long as the junctions AC and BC are both at temperature T_2, the net EMF is the same as if C were not there.*

3.4 Thermocouple compensation

It is not practical to have thermocouple cold junctions maintained at a controlled reference temperature. However, assuming that the cold junction will not change its temperature is not realistic. It is desirable to have a compensation mechanism for slight variations of the cold junction temperature around the ambient temperature level. Consider the arrangement shown in Figure 7, which is showing a thermocouple with its measuring junction at $t\,^{\circ}$C and its cold junction at ambient temperature. The bridge includes a thermistor R_t and fixed resistors R_1, R_2, and R_3. The bridge is first balanced when all of the components are at 0 °C. As the ambient temperature is changed away from 0 °C an unbalance voltage will be generated across CD. This voltage is used in the compensation of the cold junction.

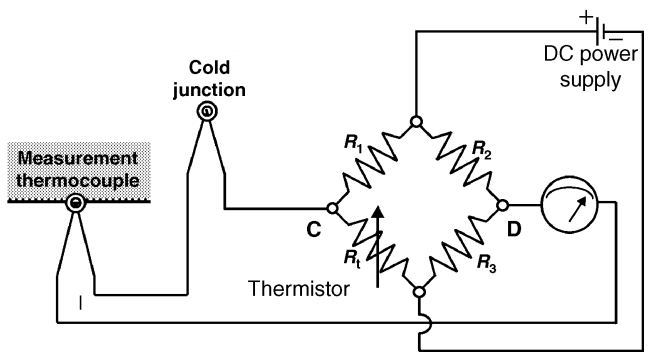

Figure 7. Cold junction compensation of a thermocouple.

3.5 Multiple thermocouple arrangements

A number of thermocouples may be connected in series or parallel as shown in Figure 8 to achieve a thermopile or an averaging system. The series arrangement is used for enhancing the sensitivity and usually termed as a "thermopile". All of the measuring junctions are held at one temperature T_1, and all of the reference junctions are exposed to another temperature T_2. Since n thermocouples are connected in a series arrangement, a thermopile gives an output n times as great as that which can be obtained from a single sensor.

The averaging circuit shown in Figure 8b generates about the same voltage level of a single thermocouple if all of the measuring junctions are kept at a common temperature. When the measuring junctions T_1, T_2, and T_3 are at different temperatures and they have the same resistance, the output voltage is the average of the voltages generated by T_1, T_2, and T_3.

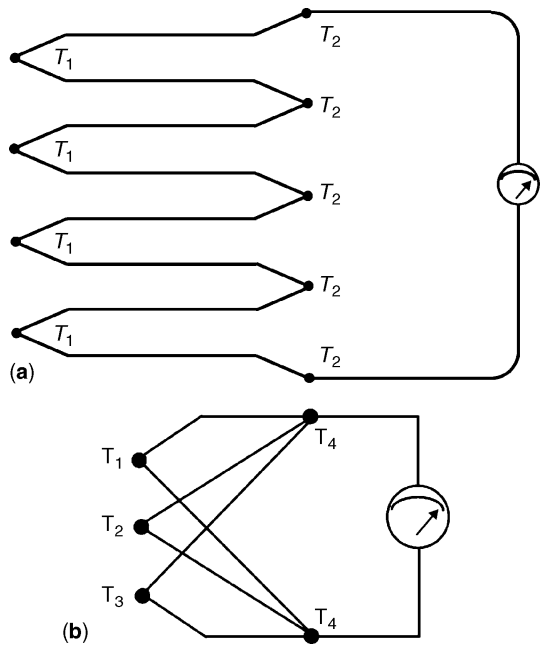

Figure 8. (a) A serial thermopile and (b) averaging with parallel connected thermocouples.

3.6 Special purpose thermocouples

Figure 9 shows three implementations of thermocouples in high-temperature rocket engine research at NASA Laboratories (Moeller, Noland and Rhodes, 1968).

4 BI-METALLIC TEMPERATURE SENSORS

Bimetallic temperature sensors are obtained by bonding together two metals with different coefficients of thermal expansion. Typical bimetallic strip materials are brass and invar. As the temperature of the bimetallic system varies, the brass side expands or contracts more than the invar, resulting in a measurable change of curvature. This temperature change will deflect the strip to form a uniform circular arc. Turner and Hill (1999) expressed the radius of curvature r as a function of m (the thickness ratio, $m = t_B/t_A$), t (the total strip thickness), and n (the ratio of elastic moduli E_B/E_A):

$$r \approx \frac{(n+1)\,t}{3n(\alpha_A - \alpha_B)(T_2 - T_1)} \tag{3}$$

In equation (3), t_B, and t_A are the thicknesses of strips A and B and $(T_2 - T_1)$ is the temperature rise influencing the bimetallic strip. In most of the practical cases $m = t_B/t_A = \sim 1$ and $(n+1)/n = \sim 2$. α_A and α_B are accurately known coefficients of thermal expansion for the two strips. Bimetallic devices are in general low-cost and low-accuracy temperature sensing devices.

5 DIODE-BASED TEMPERATURE SENSORS

PN junctions in silicon are popular temperature sensors due to their very low cost and easy manufacturing characteristics. It is well known that a voltage V_f has to be applied across the junction before a current flows (Turner and Hill, 1999). V_f which is often termed as "the diode voltage drop," is of the order of 600–700 mV for a silicon diode. V_f is highly temperature dependent, and is very nearly linear over the temperature range from -50 to $+150\,^{\circ}$C.

6 LIQUID CRYSTAL THERMOMETRY

Thermochromic liquid crystals respond to a local temperature change in terms of a distinct color change. The color of a liquid crystal can be used as an accurate indicator of

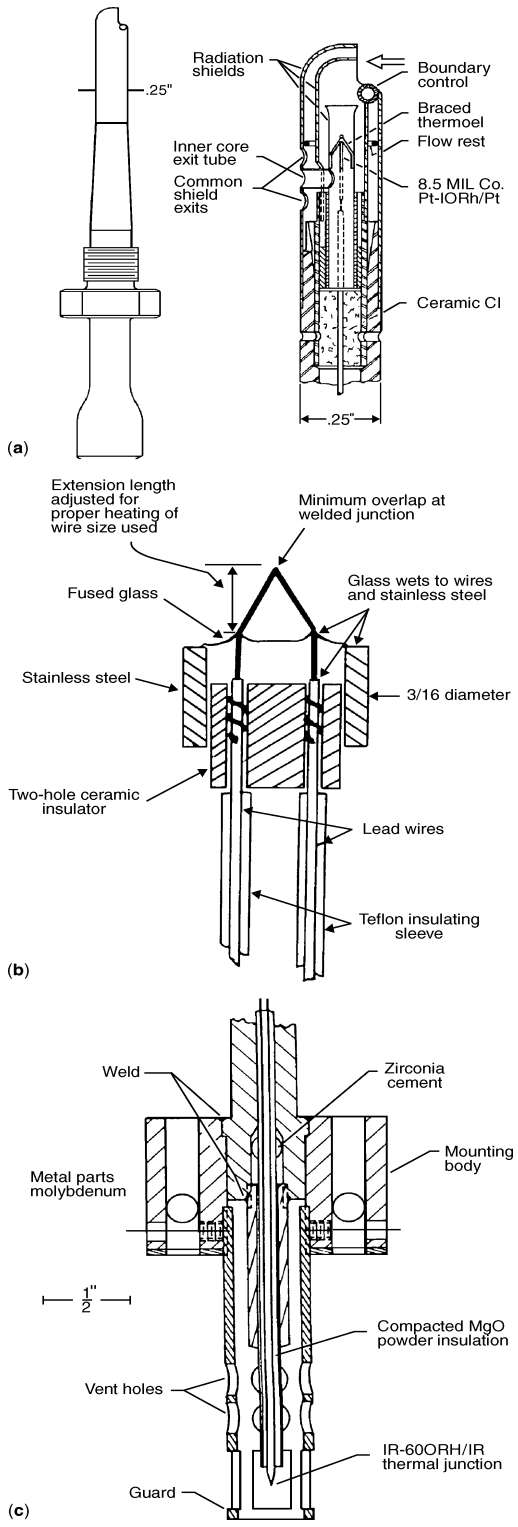

Figure 9. Special purpose thermocouples used by NASA, SP5050. (a) Fast responding shielded probe for 2700 °F operation in rocket engines, (b) probe for measuring hot hydrogen gases in the NERVA nuclear rocket, and (c) probe for measuring exhaust gases from a booster rocket. Reproduced with permission from Moeller, Noland and Rhodes (1968).

temperature. The main advantages of this technique are the direct measurement of local temperatures over the surfaces with great spatial resolution and no obstruction to the flow. Although most of the previous interpretations of the liquid crystal images are based on *human eye color perception*, which is subjective, more modern approaches implement automatic color capturing schemes for marked improvements in temperature measurement accuracy. A more comprehensive discussion of this topic by Camci, Hippenesteele and Kim (1992) and a reference list can be found (Camci, 1996).

Liquid crystals that have two distinct melting points are organic compounds derived from esters of cholesterol. At the first melting point, the solid turns to a cloudy liquid, and at the second, the liquid becomes clear. This cloudy phase, called liquid crystal phase or mesomorphic phase, is a condition intermediate between a true solid crystal and an isotropic liquid. In this phase, the molecules are movable but still organized in the form of a helical pattern. Liquid crystals are conventionally divided into three classes: smectic, chiral-nematic, and cholesteric. Cholesteric and chiral-nematic liquid crystals show a very interesting feature from a heat transfer point of view. They are relatively insensitive to normal and shearing stresses. They progressively exhibit all colors of the visible spectrum as they are heated through the event temperature range. The phenomenon is reversible and repeatable, and the color can be calibrated accurately with temperature. The color response of liquid crystals to temperature is very fast and the response time is not more than a few milliseconds. Liquid crystals are presently available for a temperature spectrum ranging from −40 to 285 °C. When the liquid crystal coated heat transfer surface is illuminated with white light, a selective reflection of a specific wavelength occurs in the helical structure of the liquid crystal.

This feature can be explained by the interference of light reflected from the helical layers so that the optical wavelength in the material actually equals the helical pitch. The pitch of the crystal helix is very sensitive to temperature, and hence the selectively reflected color may be used to indicate temperature.

An aero-thermal surface coated with a thermographic liquid crystal layer is presented in Figure 10. A liquid crystal layer is spray-painted on top of a black paint layer already existing on the heat transfer surface. Details of the conversion process from the color attributes to local temperature and the accuracy of the method are discussed in detail in Camci, Hippenesteele and Kim (1992) and Camci (1996).

Figure 11 shows a typical hue versus temperature curve for a chiral-nematic liquid crystal layer. The local temperature on the model is either recorded by a thin-foil thermocouple flush mounted underneath the liquid crystal layer or a non-intrusive infrared spot thermometer focusing on the measurement location. The local hue on the measurement

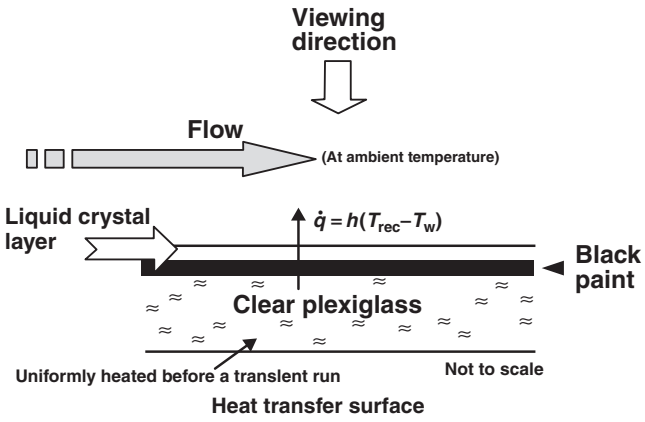

Figure 10. A liquid crystal coated aero-thermal surface for temperature measurements. Reproduced with permission from Camci (1996).

point approximately linearly varies over a temperature range where the red, green, and blue colors appear at 42.80, 43.05, and 43.30 °C, respectively. The intensity peak appearing at

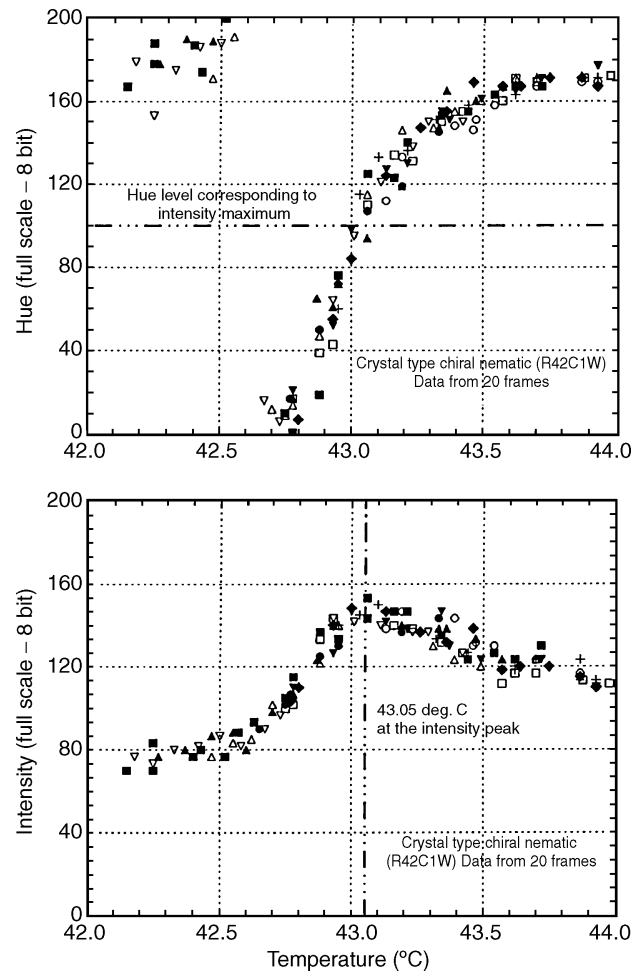

Figure 11. Liquid crystal hue and intensity as a function of the local temperature. Reproduced with permission from Camci (1992).

43.05 °C is always associated with a green color from the coated surface. The intensity attribute has a maximum in the linear part of the hue curve at about 43.05 °C. Thermally induced colors come out of a black background and transit continuously from red to blue, exhibiting a large number of hues that can be recorded by color image capturing systems.

Measured color attributes (H, S, I), measured Nusselt number distribution for a round jet impinging on a flat plate, and comparison with direct measurements using thermocouples are shown in Figure 12. The intensity distribution on the impingement plate shows two distinct peaks near $r/D = -1$ and $+1$ at a location where a green color is observed. Figure 12 indicates a good agreement between a classical thermocouple-based *Nu* measurement and the liquid crystal-based Nu measurement at $Re = 30\,000$.

Thermochromic liquid crystals have wide implementation potential for temperature measurements in a rotating frame of reference. Camci and Glezer (1997) performed a study to document the modifications of color response of liquid crystal coated surfaces when they are subject to severe centrifugal acceleration on turbine disks, rotating disks, and rotating cavities. Figure 13 presents the results of a rotating

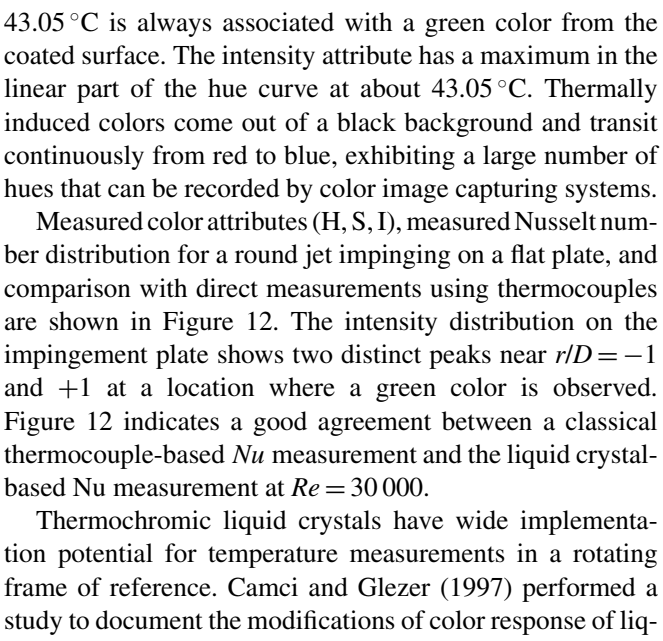

Figure 12. Liquid crystal hue and intensity as a function of local temperature and *Nu* measurement (Camci, 1992).

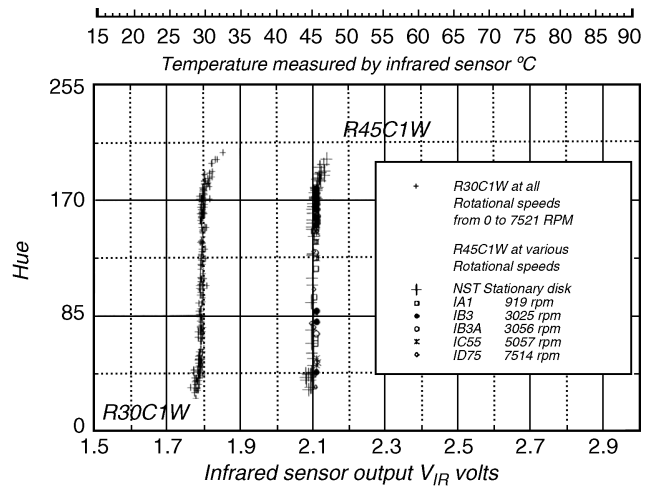

Figure 13. Liquid crystal response to centrifugal acceleration Reproduced with permission from Camci and Glezer (1997).

disk experiment with a liquid crystal coated flat surface in a rotational speed range from 900 to 7500 rpm. The disk surface temperature was non-intrusively obtained by a precision infrared measurement device at various rotational speeds. The liquid crystal hue on the disk surface is correlated with the infrared-based temperature measurement in Figure 13. It is clearly shown that the centrifugal acceleration and aerodynamic shear stress cannot alter the color response of liquid crystals in a wide centrifugal acceleration range (Camci, 1996, 1997; Camci and Glezer, 1997; Camci *et al*., 1998).

7 INFRARED THERMOMETRY AND PYROMETER

Infrared thermometers measure local temperature using blackbody radiation in the infrared range. The infrared range is just above the visible spectrum ranging from 0.4 to 0.8 μm (Balageas, 1993; Carlomagno, 1993). Generally speaking, the higher the temperature of an object, the more the infrared radiation it emits as blackbody radiation. By knowing the amount of infrared energy emitted by the object and its local emissivity characteristics, the object's local temperature or its surface temperature distribution can be determined. Typical infrared thermometer design consists of a lens to focus the incoming infrared energy onto an IR detector. This approach facilitates a non-intrusive temperature measurement from a distance without contact with the object to be measured. The infrared thermometers are extremely useful for measuring temperature under circumstances where thermocouples or other probe type sensors cannot be used or do not produce accurate data for a variety of reasons.

A typical infrared system may have an adjustable emissivity setting, which can be set to measure the temperature of reflective and non-reflective surfaces. The most common infrared thermometers are the following:

– Spot infrared thermometer, or infrared pyrometer, measures the temperature on a spot on a surface.
– Infrared line scanning systems, which scan a larger area, use what is essentially a spot thermometer pointed at a rotating mirror. These devices are widely used in manufacturing involving conveyors or web processes, such as large sheets of glass or metal exiting an oven, fabric and paper, or continuous piles of material along a conveyor belt.
– Infrared cameras are essentially infrared thermometers that measure the temperature at many points over a relatively large area to generate a two-dimensional image, with each pixel representing a temperature measurement.

An infrared scanning system may use two oscillating mirrors that define the image line by line. If the vertical scanning mirror is held at a fixed position, the relatively higher oscillating frequency of the horizontal line-scanning mirror increases the temporal measurement resolution of the IR system significantly.

A slightly different scanning system using two rotating prisms with a single IR detector is also available. More modern IR systems contain multiple rows of IR sensor arrays manufactured as charge-coupled devices. This technology is more processor- and software-intensive than spot or scanning thermometers, and is used for monitoring large areas. Cooled detectors are typically contained in a vacuum-sealed case or flask and cryogenically cooled. This greatly increases their sensitivity since their own temperatures are much lower than that of the objects from which they are expected to detect radiation. Typical cooling temperatures range from 4 to 110 K.

Without cooling, these sensors would be "blinded" or "flooded" by their own radiation. The drawbacks of cooled infrared cameras are that they are expensive both to produce and to run. Although the components that lower the temperature and pressure are generally bulky and expensive, cooled infrared cameras provide superior image quality compared to uncooled ones. A more comprehensive discussion on IR temperature measurement systems is given in Arts and Charbonnier (1994) and Simeonides *et al*. (1991).

8 HEAT TRANSFER MEASUREMENTS

Measurements of convective, conductive, radiative, or total heat transfer rates are often required in aerospace engineering such as atmospheric re-entry studies, hot section component development for gas turbines, ramjet/scramjet development, ballistic missile nose cone development, heat exchanger development, rocket engine combustors, and nozzles. Figure 14 gives the most frequently employed methods of heat transfer measurements in aerospace engineering.

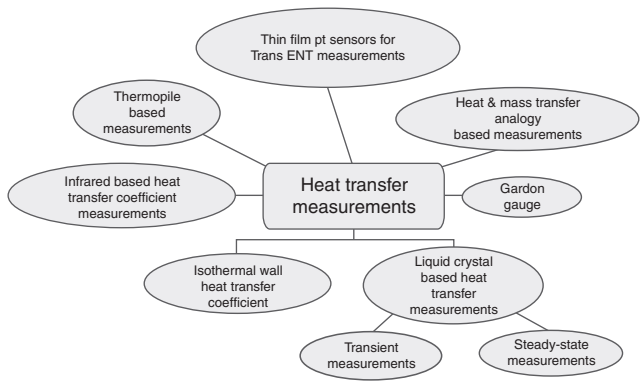

Figure 14. Various heat transfer measurement approaches in aerospace engineering.

The simplest steady-state heat flux sensor can be constructed from two temperature-sensing elements that are physically separated by a material with known thermal conductivity. The temperature gradient provided by the two sensors, the thickness of the material between the two sensors, and the thermal conductivity of the material can provide an accurate measurement of the unidirectional heat flux.

In addition to steady-state heat flux sensors, special unsteady heat flux sensors are also used for time-accurate measurements. For example, the local convective heat transfer rate measured on the surfaces of a gas turbine blade located at just downstream of a nozzle guide vane is highly rotor position dependent and inherently unsteady (Dunn, 1984). The blade surfaces are exposed to highly fluctuating rates of heat transfer when they pass through the individual wakes of the nozzle guide vanes. In a transonic turbine blade, heat transfer sensors may also see the passage of shockwaves as strong/unsteady variations of convective heat transfer rates (Asworth *et al*., 1985; Camci and Arts, 1985).

The heat transfer rates occurring during the re-entry of space vehicles are usually simulated in hypersonic long-shot facilities where thin-film platinum sensors or infrared sensors are used as unsteady temperature sensors (Schultz and Jones, 1973). This approach assumes a one-dimensional flow of heat into a semi-infinite substrate at the fluid–solid interface. The output of a platinum sensor or the infrared camera can be used to obtain an accurate wall heat flux measurement using the analytical and numerical methods discussed in Camci and Arts (1985), and Schultz and Jones (1973). The total time

duration of a short-duration heat transfer experiment ranges from microseconds to milliseconds, where time-accurate and fast wall temperature sensing and use of "analog circuits" or "equivalent computer algorithms" in the construction of a heat flux signal are essential.

A time-accurate heat flux sensor can also be obtained by depositing two nickel thin-film temperature sensors on either side of a thin insulator. A very high frequency response of this type of heat flux sensor allows measurement of unsteady wall heat flux at 200 000 Hz (Guenette *et al*., 1989). Instead of using just one deposited nickel temperature sensor on both sides of an insulator, one may effectively use a thermopile of thin-film deposited thermocouples in the construction (Holmberg and Diller, 1995). General aspects of thin-film sensor-based unsteady heat transfer measurements are discussed in Camci and Arts (1985), Doorly and Oldfield (1985), Dunn, Martin and Stanek (1986), and Abhari and Epstein (1994). A comprehensive review of the general heat transfer measurements used for the turbine hot-section aerothermal research can also be found in Han, Dutta and Ekkad (2000). Liquid crystal thermography can also be implemented into heat transfer experiments for the purpose of obtaining convective heat transfer rates as discussed in Camci (1996) and Han, Dutta and Ekkad (2000).

Heat/mass transfer analogy is a frequently used method of measuring local heat transfer coefficients on fluid–solid interfaces. Mass-transfer analogy approach provides high resolution measurements with almost no heat loss, and reduced axial conduction effects in low-speed wind tunnel environment. Naphthalene sublimation method was extensively used in the past to study heat/mass transfer characteristics on turbine blades, endwall boundary layers, and cooled film surfaces (Goldstein and Taylor, 1982; Goldstein and Spores, 1988; Han, Chandra and Lau, 1988). Swollen polymer technique is another mass transfer-based heat transfer measurement approach that can be combined with laser holographic interferometry to obtain fairly detailed heat transfer measurements resulting in an uncertainty of about 3%. A review of other mass transfer-based heat transfer methods such as ammonia-diazo technique, pressure sensitive paint, and foreign gas concentration sampling is presented in Han, Dutta and Ekkad (2000).

9 CONCLUSIONS

This chapter is limited to the discussion of the most frequently used temperature and heat transfer measurement methods in aerospace engineering. Thermographic phophors as temperature-sensitive paints are excluded from this discussion. Although many illustrations and discussions are used throughout the text, more detailed information in this area can be obtained from many references provided.

ACKNOWLEDGMENTS

The author acknowledges the invaluable support of S.A. Hippensteele of NASA Glenn/Lewis Research Center, Dr. Boris Glezer of Solar Turbines, Inc., and the Department of Aerospace Engineering at Pennsylvania State University, for the sponsorship and technical help provided for the author's liquid crystal thermography research. He also acknowledges the valuable contributions made by Dr. Kuisoon Kim of Pusan National University, Korea, Dr. Brian Wiedner, Dean Rizzo, and Dr. Oguz Uzol of the Middle East Technical University, Ankara.

REFERENCES

Abhari, R.S. and Epstein, A.H. (1994) An experimental study of film cooling in a rotating transonic turbine. *ASME J. Turbomach.*, **116**, 63–70.

Arts, T. and Charbonnier, J.M. (1994) Temperature measurements, in *von Karman Institute Lecture Series on Introduction to Measurement Techniques*, 1994-01.

Asworth, D.A., LaGraff, J.E., Schultz, D.L. and Grindrod, K.J. (1985) Unsteady aerodynamic and heat transfer processes in a transonic turbine stage. *ASME J. Eng. Gas Turbines Power*, **107**, 1022–1030.

Balageas, D.L. (1993) Fundamentals of Infrared Thermography, in *von Karman Institute Lecture Series on Measurement Techniques*, 1993-05.

Camci, C. and Arts, T. (1985) Short duration heat transfer measurements, in *von Karman Institute Lecture Series on Measurement Techniques in Turbomachines*, 1985-03.

Camci, C. and Arts, T. (1985) Theoretical and experimental investigation of film cooling heat transfer on a gas turbine blade. Ph.D. Thesis. von Karman Institute for Fluid Dynamics and Katholieke Universiteit, Leuven, Belgium.

Camci, C., Hippensteele, S.A. and Kim, K. (1992.) A new hue capturing technique for the quantitative interpretation of liquid crystal images used in convective heat transfer studies. *ASME J. Turbomach.*, **114**(4), 765–775.

Camci, C. (1996) Introduction to liquid crystal thermography and color recognition for temperature measurements on liquid crystal coated surfaces, in *von Karman Institute Lecture Series on Temperature Measurements*, VKI-LS-1996-09.

Camci, C. and Glezer, B. (1997) Liquid crystal thermography on the fluid–solid interface of rotating systems. *ASME J. Heat Transfer*, **119**(1), 20–29.

Camci, C. (1997) Liquid crystal thermography on the rotating surfaces of turbomachinery systems, in *Advanced Turbomachinery*

Design (ed. C. Hah), Marcel Dekker Inc., New York, ISBN: 9780824798291.

Camci, C., Owen, J.M., Pilbrow, R.G. and Syson, B.J. (1998) Application of thermochromic liquid crystal to rotating surfaces. *ASME J. Turbomach.*, **120**(1), 100–103.

Carlomagno, G.M. (1993) Infrared Thermography, in *von Karman Institute Lecture Series on Measurement Techniques*, 1993-05.

Doorly, D.J. and Oldfield, M.L.G. (1985) Simulation of effects of shock waves passing on turbine rotor blade. *ASME J. Eng. Gas Turbines Power*, **107**, 998–1006.

Dunn, M.G. (1984) Turbine heat flux measurements: influence of slot injection on vane trailing edge heat transfer and influence of rotor on vane heat transfer. ASME Paper 84-GT-175.

Dunn, M.G., Martin, H.L. and Stanek, M.J. (1986) Heat flux and pressure measurements and comparison with prediction for a low aspect ratio turbine stage. *ASME J. Turbomach.*, **108**, 108–115.

Goldstein, R.J. and Taylor, J.R. (1982) Mass transfer in the neighborhood of jets entering a crossflow. *ASME J. Heat Transfer*, **104**, 715–721.

Goldstein, R.J. and Spores, R.A. (1988) Turbulent transport on the endwall in the region behind adjacent turbine blades. *ASME J. Heat Transfer*, **110**, 862–869.

Guenette, G.R., Epstein, A.H., Giles, M.B. *et al*. (1989) Fully-scaled transonic turbine rotor heat transfer measurements. *ASME J. Turbomach.*, **111**, 1–7.

Han, J.C., Chandra, P.R. and Lau, S.C. (1988) Local heat/mass transfer distributions around sharp 180° turns in two pass smooth and rib roughened channels. *ASME J. Heat Transfer*, **110**, 91–98.

Han, J.C., Dutta, S. and Ekkad, S.V. (2000) *Gas Turbine Heat Transfer and Cooling Technology*, Taylor & Francis, NY, ISBN # 1-56032-841-X.

Holmberg, D.G. and Diller, T.E. (1995) High-frequency heat flux sensor calibration and modeling. *ASME J. Fluid. Eng.*, **117**, 659–664.

Moeller, C.E., Noland, M. and Rhodes, B.L. (1968) NASA Contributions to Development of Special Purpose Thermocouples, A Survey, *NASA SP-5050*.

Moffat, R.J. (1962) The gradient approach to thermocouple circuitry, in *Temperature – its Measurement and Control in Science and Industry*, vol. 3, Part 2, Reinhold, New York.

Rogers, G.F.C. and Mayhew, Y.R. (1983) *Engineering Thermodynamics, Work and Heat Transfer*, 3rd edn, Longman.

Schultz, D.L. and Jones, T.V. (1973) Heat Transfer Measurements in Short Duration Hypersonic Facilities, *Agardograph AG-165*.

Simeonides, G., Vermeulen, J.P., Boerrigter, H.L. and Wendt, J.F. (1991) Quantitative heat transfer measurements in hypersonic wind tunnels by means of infrared thermography, in *ICIASF '91, International Congress on Instrumentation in Aerospace Simulation Facilities, Rockville, MD*.

Turner, J. and Hill, M. (1999) *Instrumentation for Engineers and Scientists*, Oxford Science Publications.

Yang, T.T. and Diller, T.E. (1995) Heat Transfer and Flow for a Grooved Turbine Blade Tip in a Transonic Cascade, ASME Paper 95-WA/HT-29.

Q1

Abstract:
This chapter deals with the state-of-the-art in temperature and heat transfer measurements that are frequently encountered in Aerospace Engineering. Resistive temperature transducers, thermocouples, bi-metallic temperature sensors, semi-conductor diode-based temperature sensing, liquid crystal thermography, infrared thermography, and pyrometry are discussed in detail. Measurements of convective, conductive, radiative, or total heat transfer rates are often required in aerospace engineering such as atmospheric re-entry studies, hot-section component development for gas turbines, ramjet/scramjet development, ballistic missile nose cone development, heat exchanger development, rocket engine combustors, and nozzles. Finally, heat transfer measurements are discussed. Although many illustrations and discussions are used throughout the text, more detailed information in this area can be obtained from the many valuable references provided.

Keywords: temperature, heat transfer, thermocouples, liquid crystals, infrared sensors, pyrometer

Author Query

[**Q1**] Please provide citation of Yang T.T. (1995) in text or this can be moved to the Further Reading Section.